OPTIMISATION OF THE INDUSTRIAL COMPUTED RADIOGRAPHY USING THE SIGNAL DIFFERENCIAL-TO-NOISE RATIO (SdNR)

Aline Saddock, David F. Oliveira and Ricardo T. Lopes
Federal University of Rio de Janeiro (UFRJ/COPPE)
Laboratory of Nuclear Instrumentation

Abstract

The transition from analog to digital operation that the radiography has experienced has provided new and important challenges in the way the images are acquired and displayed. There are several digital image acquisition systems, as for example, the computerized system, which uses Image Plates (IP). A methodology for the evaluation of image quality is through the parameter signal differential-to-noise ratio (SdNR). This parameter allows correlating the signal and the noise to the visualization of image details, allowing not only the evaluation of the signal noise ratio (SNR), but also how the rate interferes with the image. Thus, the greater the SdNR, the greater will be the visualization quality of details on the image. However, in order to compare different radiographic techniques through this system it is also necessary to calculate the Figure of Merit (FOM), that in this in case, it is given by the square of the SdNR per unit of applied dose. The IP was used in the accomplishment of this work with the aim to study a technique capable of optimizing the acquisition of digital image. The method proposed in this work is about the use of IP to carry out SdNR experimental measurements and consequently FOM measurements in applications of the x-ray of pieces in aluminum and iron. This proceeding was done varying some specific parameters of the system, as high voltage, exposition and the use of filters in the X-rays tube exit. As a result, an SdNR was obtained for each technique allowing in this way to verify the behavior of the FOM in each one of them.

1. Introduction

In the last years, radiography has experienced a transition from analog to digital operation, since the digital radiography has facilitated an operational convenience that was not previously possible with analog systems. The use of the digital radiography in the industrial area played an important role for the development of the quality control in diverse industrial processes, such as weld inspection and analysis of corrosion.

Nowadays, there are several systems of digital image acquisition, such as Image Plates (IPs). The IPs are made of special phosphors that capture and “store” radiation. They are placed in a cassette or used in their original flexible state and when exposed to radiation a latent image is created. That latent image is then “read” by the CR scanner. A laser beam in the CR reader excites the energy stored on the plate, and the visible energy released is captured as a digital mage. This process is known as photostimulated luminescence.

On these plates, the image acquisition occurs in two stages. Firstly, the creation of the latent image occurs and afterwards the transformation of the latent image into radiographic image.

The creation of latent image in IP is based on the electron energy. In the process for obtention of phosphorus, impureness or activators that create energy levels between valence and conduction band, called F-centers or color centers, are introduced into the crystal. With the exposure of phosphorus particles to ionizing radiation, the excited electrons pass to a higher energy level leaving behind a lacuna on the Eu^{2+} ion. While some of these electrons immediately recombine themselves and excite the Eu^{2+}, which promptly start emitting radiation, the others keep trapped in the F-centers. The stored energy in these pairs electron-lacuna is the base of the latent image, which conserves itself relatively stable for several hours.

The transformation of the latent image into radiographic image is generally done through red laser (700 nm). It is used to stimulate the phosphorous in a way that it allows releasing its stored energy under visible light – PSL, whose intensity is directly proportional to the number of X rays photons absorbed by the storing phosphorous. These photons are conducted through a light guide to a photomultiplier where they are transformed into an electronic signal that is amplified and conducted over a digital to analog converter. At last, as a result, the pixels are assembled in the same radiographic image.

Utilization of IPs has introduced new and important changes in the way digital images are acquired and presented and thus bringing out an improvement of the image quality. When compared to conventional films its characteristics are quite superior: highly sensitiveness; high dynamic range; superior linearity; good spatial resolution; besides the fact that the digital data are directly obtained from the computer for image treatment.

A way to evaluate the quality of the digital image is the signal differential-to-noise ratio (SdNR). This magnitude was suggested by Samei et al. [1], in 2005, to investigate medical digital images. The SdNR allows correlating the signal and the noise to the visualization of the image details, allowing not only the evaluation of the signal noise ratio (SNR), but also how this rate is interfering in the image. Thus, the larger the SdNR, the larger will be the visualization quality of details on the image.

However, in order to compare different radiographic techniques through this system it is also necessary to calculate the Figure of Merit (FOM), that in this in case, it is given by the square of the SdNR per unit of dose. Therefore, the purpose of this paper is to describe a simple experimental approach that can be used for technique optimization of digital radiographic systems.

2. Optimization Method

The SdNR is used to compare the visualization of details in the image obtained through different radiographic techniques. For each image, the specific regions of interest (ROIs) defining various details and the background should be identified. Figure 1 illustrates a digital image of a phantom constituted by a detail in the background.

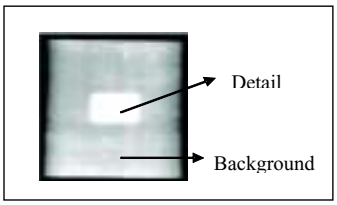

Figure 1. Phantom digital image.

When the details are in the background, the single-exposure method is used and when they are not the dual-exposure method is used. For the single-exposure method the SdNR is defined as:

$$SdNR = \frac{< L(i,j) > - < B(m,n) >}{\sigma_B} \tag{1}$$

where ***L(i,j)*** and ***B(m,n)*** refer to small ROIs defined within the areas of the detail and the background, respectively and σ_B is the standard deviation of detector noise in the background.

The contrast is defined as:

$$C = \frac{\langle L(i,j)\rangle - \langle B(m,n)\rangle}{\langle B(m,n)\rangle} \tag{2}$$

Using the dual-exposure method, the SdNR is defined as:

$$SdNR = \frac{\left\langle \frac{1}{\beta}\left[L_{W0}(i,j) - L_W(i,j)\right]\right\rangle}{\sigma_B} \tag{3}$$

where $L_{W0}(i,j)$ and $L_W(i,j)$ refer to a small ROI defined within the areas of the detail. ***W*** and W_0 refer to the images with and without the details, respectively. Noise is computed as:

$$\sigma_B = \frac{\sqrt{\frac{1}{(ixj)-1}\sum_{i,j}\left(B'(i,j) - \langle B'(i,j)\rangle\right)^2}}{\sqrt{1+\beta^{-2}}} \tag{4}$$

where: $$B'(i,j) = \frac{1}{\beta}B_{W0}(i,j) - B_W(i,j) \tag{5}$$

and $$\beta = \left\langle \frac{B_{w0}(i,j)}{B_w(i,j)} \right\rangle \tag{6}$$

where $B_{W0}(I,j)$ e $B_W(I,j)$ refers to a small ROI defined within the areas of the background.

In this case, the contrast is defined as:

$$C = 1 - \beta\left\langle \frac{L_w(i,j)}{L_{w0}(i,j)} \right\rangle \tag{7}$$

The FOM is calculated as:

$$FOM = \frac{SdNR^2}{E} \tag{8}$$

where E is the estimated exposure at the plane of the reference.

The SdNR and FOM figures calculated above have contribution of scattered radiation. The calculated SdNR associated only with the primary radiation is defined as:

$$SdNR_p^2 = \frac{SdNR^2}{1 - SF} \tag{9}$$

SF is the scatter fraction defined as:

$$SF = \beta\left\langle \frac{A_W(i,j)}{A_{W0}(i,j)} \right\rangle \tag{10}$$

where $Awo(i,j)$ and $Aw(i,j)$ refers to a small ROI defined within the *beam-stop* area.

To compare two distinct techniques it is done the ratio among the FOMs of the radiographic techniques:

$$nFOM = \frac{FOM_2}{FOM_1} \tag{11}$$

where FOM_1 and FOM_2 are FOM values for the techniques 1 and 2, respectively.

When the nFOM is higher than 1 it means that technique 2 was capable of increasing the SdNR or diminishing the exposure. The increase in SdNR means that with this technique it is possible to get a better visualization on the image details and the decrease of exposure means that this technique requires less exposure to be performed.

3. Materials and Methods

In this work it was used a X-ray tube, the IP, a computerized radiography system CR Tower Scanner – GE and the Rhythm Acquire and Review programs for image acquisition and treatment, respectively. The Image Plate was placed at 1 m of the X-ray tube.

As the focus of this work is on the application of digital radiography in industry, a phantom was used to simulate proper characteristics of such area, or rather, a piece that had lack and excess of the same material. Thus, two phantoms were prepared and analyzed: aluminum and iron phantoms (Figure 2).

The aluminum phantom (Al) is a plate of 10mm of thickness, with four grooves and four aluminum pieces positioned above it. The grooves are 1, 2, 3 and 4 mm of depth (Figure 2 (a) – details 1, 2, 3 and 4 respectively) and pieces of 1, 2, 3 and 4 mm of thickness (Figure 2 (a) – details 5, 6, 7 and 8, respectively). A piece of lead (Figure 2 (a) – detail 9) of 20 mm of thickness, called beam-stop, was set on its centre in order to correct the influence of the scattered radiation by the material.

The iron phantom (Fe) was prepared like the aluminum phantom. It consists of a plate of 6 mm of thickness, with four grooves and four iron pieces positioned above it. The grooves are 1, 2, 3 and 4 mm of depth (Figure 2 (b) – details 1, 2, 3 and 4 respectively) and pieces of 1, 2, 3 and 4 mm of thickness (Figure 2 (b) – details 5, 6, 7 and 8, respectively). Like the aluminum phantom, the beam-stop (Figure 2 (b) – detail 9) was set on its center.

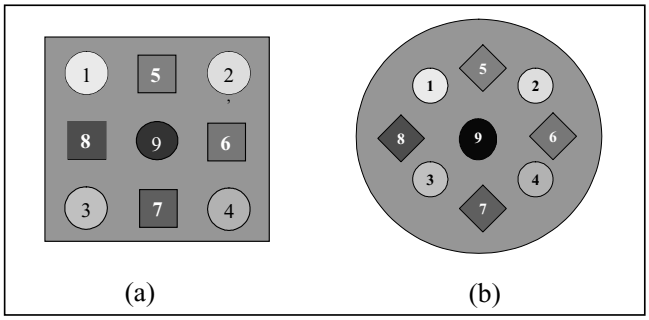

Figure 2. Project of (a) aluminum and (b) iron phantom used.

The methodology of this work is to carry out several exposition of the phantom varying the parameters of the system. To both phantoms, the applied high voltage, the selected current, the exposure time, the filter set in front of the X-Rays tube and the IP were varied. It was used three different IPs: IPC, IPX and IPS. The measurements were carried out in a way that for each parameter that was varied, the others were kept constant.

For the aluminum phantom, the applied high voltage varied from 30 to 50 kV in steps of 5 kV, the current from 1 to 5 mA in steps of 1mA and the time from 10 to 50 s in steps of 10 s. Copper and aluminum filters with 1.7 to 5.1 mm and 1.7 to 5.9 mm of thickness were used, respectively.

For the iron phantom, the applied high voltage varied from 80 to 100 kV in steps of 5 kV, the current from 2 to 5 mA in steps of 1mA and the time from 10 to 50 s in steps of 10 s. Copper filters with 0.5 to 2.1 mm of thickness were used.

When the measurements were carried out and the image acquisition were done, the SdNR value was obtained for each technique, thus allowing to verify the behavior of the FOM in each one of them, or rather, making possible to evaluate how each parameter of the measurement system may affect the FOM.

3. Results

The radiographic images of the analyzed phantom were obtained as result of the digital radiographic technique. With these images it was possible to obtain the FOM values in each technique. To analyze the results, demonstrative graphics of the FOM behavior in function of variation of each parameter of the measurement system were done. With the purpose of analyzing this behavior, two curves were done for each varied parameter, one for the inserted details and other for the non-inserted details.

The obtained results for the aluminum phantom are shown on graphics in Figures 4-9 and for the iron phantom in Figures 11-14. A first comment is that in all the graphics presented the FOM increases with the thickness of the detail, or rather, the higher the depth on the inserted details, or the height of the non-inserted ones, the higher the FOM value will be.

3.1 Aluminum Phantom

Figure 3 shows two images of aluminum phantom. A comparison is done between the acquired images through the optimized method (a) and the non-optimized method (b) making clear the advantage of using such method.

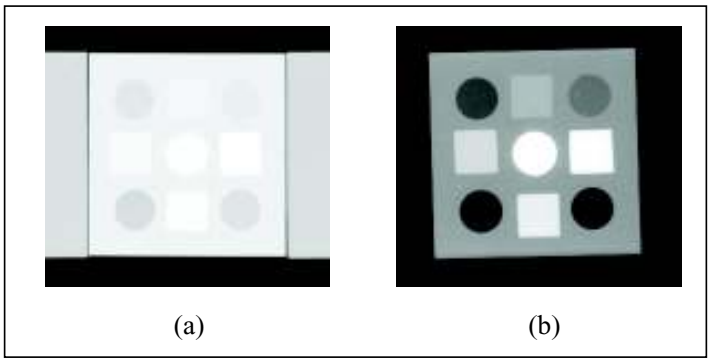

Figure 3. Images of aluminum phantom with the (a) non-optimized and (b) optimized method.

In Figure 4 it is shown the graphics of the FOM variation with an applied high voltage to the system. For the inserted details (a), the FOM reaches its maximum value in 35 kV. But for the non-inserted details (b), this value is reached for a greater high voltage value (50 kV).

The curves of FOM variation with the current are shown in Figure 5. As for the inserted details (a) as for the non-inserted details (b) the FOM is higher for a current of 4 mA. In this case, the current is high enough to visualize the details but it is low enough to not present elevated dose levels.

In Figure 6 it is shown the graphics of the FOM variation with the exposure time for the inserted details (a) and non-inserted ones (b). In both cases the FOM increases with the exposure time, reaching the maximum value in 40 s. Therefore, although the dose increases with the time growth, the acquired image in the highest time was the one that had a better consideration between image quality and dose.

The FOM variation with the thickness of the copper filter is shown in Figure 7. Despite the dose level being proportional inverse to the thickness of the filter, either for

the inserted details (a) or for the non-inserted ones (b), the FOM is higher for low values of thickness.

Figure 8 shows the FOM variation with the thickness of the aluminum filter. Its maximum value is reached at 4.2mm of thickness for the details that are not inserted (a) and at 3.3mm of thickness for the inserted ones (b).

The curves of FOM variation with the IP are shown in Figure 9. For the inserted details (a), the FOM reaches its maximum value for the IPS. But for the non-inserted details (b), this value is reached for the IPC. The IPC plate is more sensible than the IPS plate and therefore, the former gives a better FOM for the inserted details, since in these ones the radiation has to pass through a higher thickness of the material.

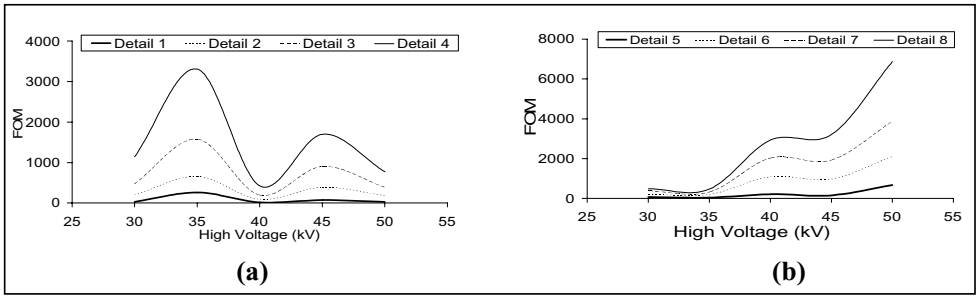

Figure 4. FOM variation with an applied high voltage for the details (a) non-inserted and (b) inserted, for the aluminum phantom.

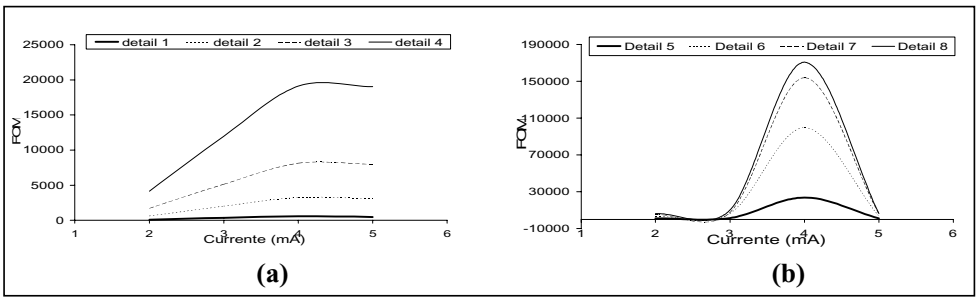

Figure 5. FOM variation with the current for the details (a) non-inserted and (b) inserted, for the aluminum phantom.

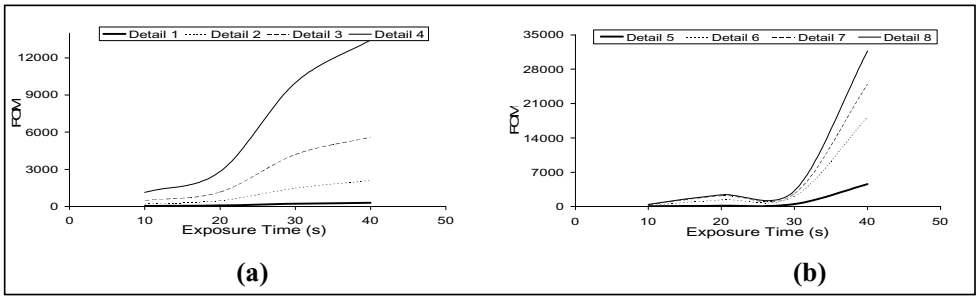

Figure 6. FOM variation with the exposure time for the details (a) non-inserted and (b) inserted, for the aluminum phantom.

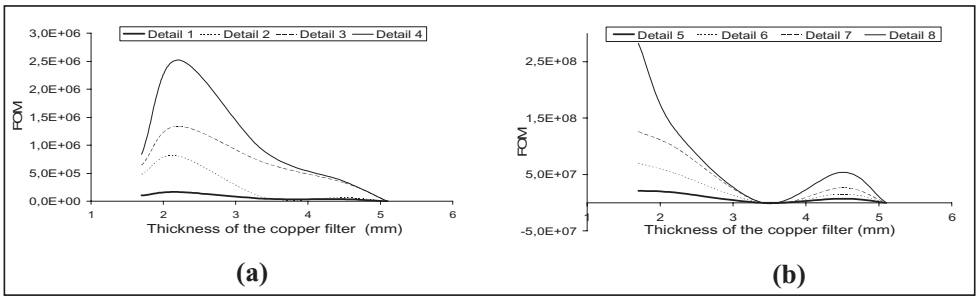

Figure 7. FOM variation with the thickness of the copper filter for the details (a) non-inserted and (b) inserted, for the aluminum phantom.

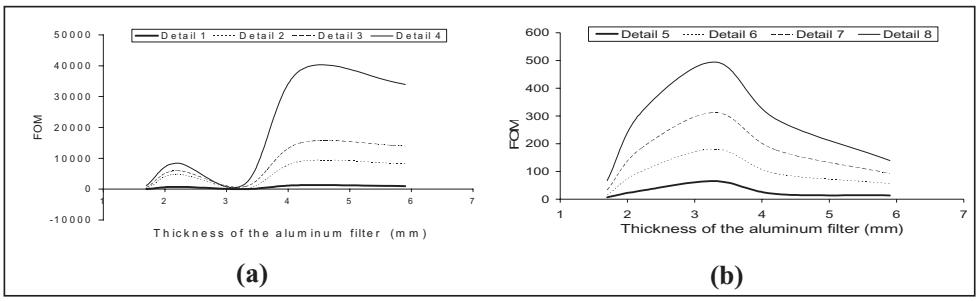

Figure 8. FOM variation with the thickness of the aluminum filter for the details (a) non-inserted and (b) inserted, for the aluminum phantom.

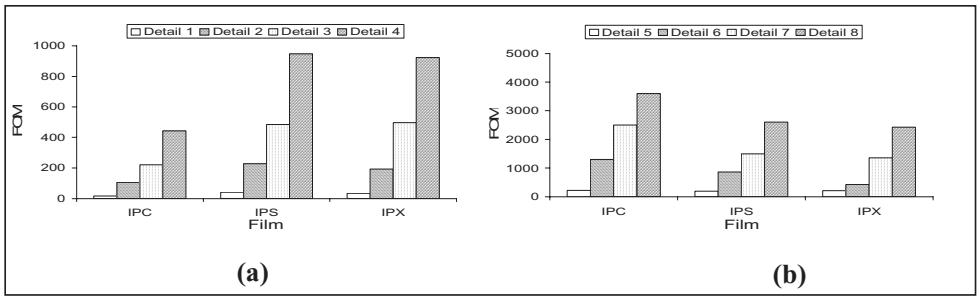

Figure 9. FOM variation with the IP for the details (a) non-inserted and (b) inserted, for the aluminum phantom.

3.3 Iron Phantom

Figure 10 shows a comparison between two images of the iron phantom obtained through the optimized method (a) and the non-optimized method (b) once more showing the advantage of this method over the first one.

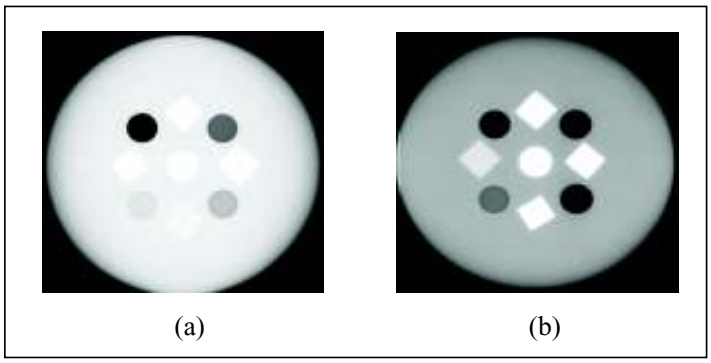

Figure 10. Images of iron phantom with the (a) non-optimized and (b) optimized method.

Figure 11 shows the FOM behavior in function of variation of tension applied to the system. For the non-inserted details (a) the FOM is higher for 95kV, as for the inserted details (b) it is higher for 85kV.

The variation curves of FOM with the current are shown in Figure 12. Either for the non-inserted details (a) or for the inserted ones (b) the FOM is higher for a current of 3mA. This can be explained is explained due to the fact that the dose is proportional to itself, or rather low current leads to low dose.

Figure 13 shows the FOM variation graphics with the exposure time. For the non-inserted details (a), the FOM reached its maximum value in 20s, as for the inserted details (b) this is reached in 30s. As the time of exposure increases the dose increases too, worsening the consideration between dose and visualization quality of details.

The FOM variation with the thickness of a copper filter is shown in Figure 14.Its maximum value is reached in 0.5mm for the non-inserted details (a) and 1.3mm for the inserted ones (b).

Figure 15 shows the variation curves of FOM with the type of IP used. Either for the non-inserted details (a) or for the inserted ones (b) the FOM is higher for the IPC plate. Such plate is more sensible than the three ones used requiring thus a lesser exposure than the others.

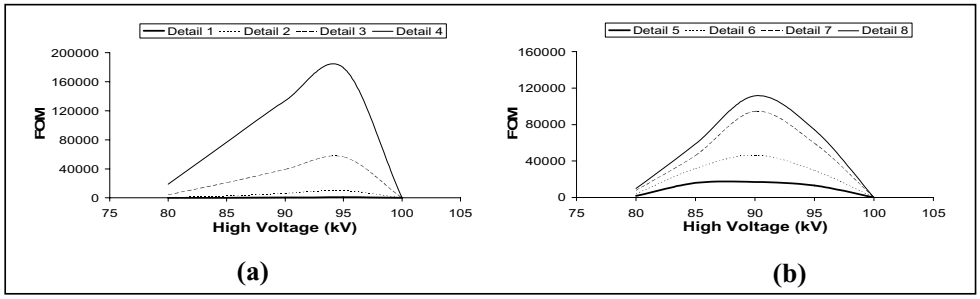

Figure 11. FOM variation with an applied high voltage for the details (a) non-inserted and (b) inserted, for the iron phantom.

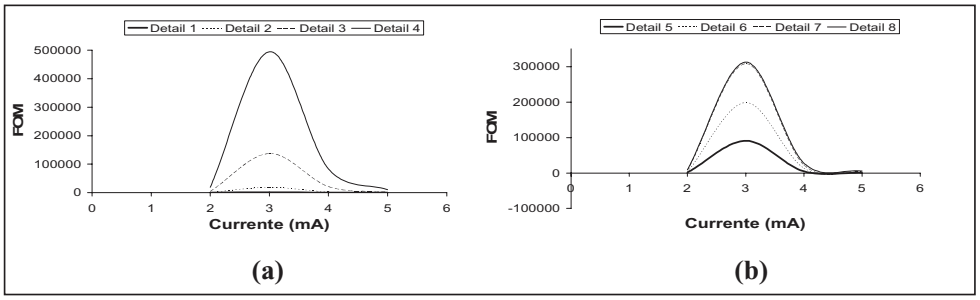

Figure 12. FOM variation with the current for the details (a) non-inserted and (b) inserted, for the iron phantom.

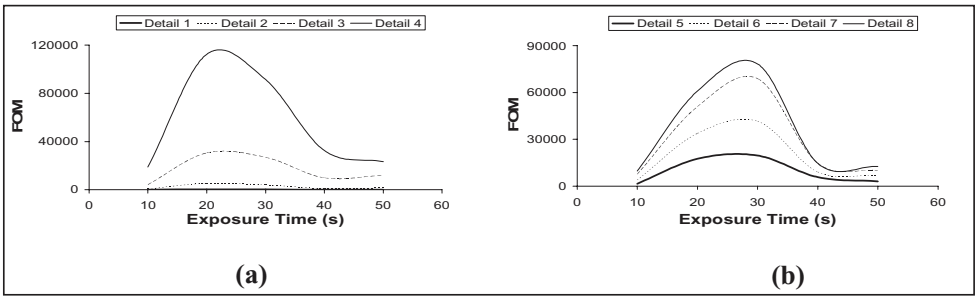

Figure 13. FOM variation with the exposure time for the details (a) non-inserted and (b) inserted, for the iron phantom.

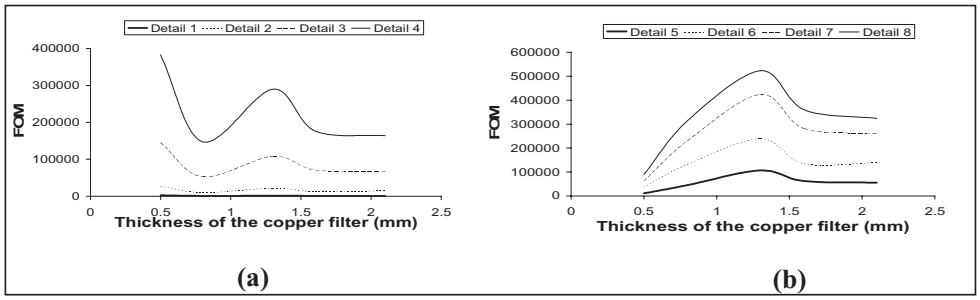

Figure 14. FOM variation with the thickness of the copper filter for the details (a) non-inserted and (b) inserted, for the iron phantom.

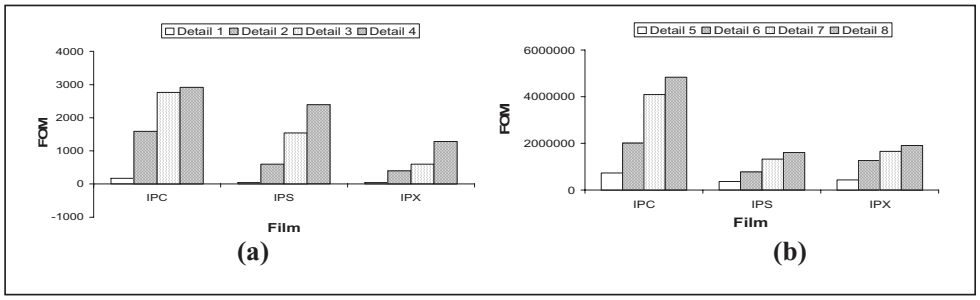

Figure 15. FOM variation with an applied high voltage for the details (a) non-inserted and (b) inserted, for the iron phantom.

4. Conclusions

The advent of the digital radiographic applied to industrial area raised the necessity of optimizing the beam quality not only to obtain a better visualization over the image details but also a reduction to the given dose to the workers. From this point, SdNR values were used to assess the image quality and FOM was used to estimate the optimization of the digital radiography based on the balance between image quality and exposure.

This work presented some digital radiographic results with the aim to evaluate the contribution of some parameters to the digital image acquisition that is adequate to industrial area, besides ensuring the safety and health of workers in this area

The obtained results in this work are coherent and therefore, they assure potentiality and feasibility on the use of this technique and emphasize the necessity of continuing the works aiming to expand knowledge over them.

Acknowledgments

This work was partially supported by Conselho Nacional de Desenvolvimento Científico e Tecnológico (CNPq) and Fundação de Amparo à Pesquisa do Estado do Rio de Janeiro (FAPERJ).

References

1. Samei, E., Dobbins, J.T., III, Lo, J. Y., Tomai, M. P., 2005, A framework for optimising the radiographic technique in digital X-ray imaging. Radiation Protection Dosimetry, Vol. 114, pp. 220-229.

2. Doyle, P., Martin, C.J., Gentle D., 2005, Dose-image quality optimization in digital chest radiography. Radiation Protection Dosimetry, Vol. 114, pp. 269-272.

3. Sandborg, M., McVey, G., Dance, D. R., Carlsson, G. A., 2001, Schemes for the optimization of chest radiography using a computer model of the patient and X-ray imaging system. Medical Physics, Vol. 28, pp. 2007-2019.

4. Lee, S.C., Wang, J.N., Liu, S.C., Jiang, S.H., 2007, Evaluation of dose-image-quality optimization in digital chest radiography. Nuclear Instruments and Methods in Physics Research A, Vol. 580, pp. 544-547.

5. Takahashi, K., 2002, Progress in science and technology on photostimulable BaFX:Eu^{2+} (X=Cl, Br, I) and imaging plates. Journal of Luminescence, Vol. 100, no. 1, pp. 307-315(9).

6. Gurvich, A. M., Hall, C., Kamenskikh, A., Munro, H., Mikhailin, V. V., Worgan, J. S., 1996. Phosphors for Luminescent Image Plates. Journal of X-Ray Science and Tecnology, 6, 48-62, article no. 0003.